Wood Flour/Polylactide Biocomposites Toughened with Polyhydroxyalkanoates

Tao Qiang,[1,2] Demei Yu,[1,3] Honghong Gao[4]

[1]*Ministry of Education Key Laboratory for Nonequilibrium Synthesis and Modulation of Condensed Matter, School of Science, Xi'an Jiaotong University, Xi'an 710049, China*
[2]*School of Materials and Chemical Engineering, Xi'an Technological University, Xi'an 710032, China*
[3]*Key Laboratory of Electrical Insulation and Power Equipment, Xi'an Jiaotong University, Xi'an 710049, China*
[4]*School of Mechanical and Electrical Engineering, Xi'an Technological University, Xi'an 710032, China*

Received 17 January 2010; accepted 7 July 2011
DOI 10.1002/app.35224
Published online 21 October 2011 in Wiley Online Library (wileyonlinelibrary.com).

ABSTRACT: Polylactide (PLA)-based wood–plastic composites (WPCs) were successfully manufactured by extrusion blending followed by injection molding. The effects of polyhydroxyanoates (PHAs) on the mechanical and thermal properties and the morphologies of the PLA-based WPCs were investigated with mechanical testing, thermal analysis, and scanning electronic microscopy (SEM). The inclusion of PHAs in the PLA-based WPCs produced an increase in the impact resistance and a decrease in the tensile strength. The brittle–ductile transition of the impact strength for the PLA-based WPCs toughened with PHAs was confirmed when the wood flour content was between 15 and 35 wt %. SEM images showed that the fracture surfaces of the PLA-based WPCs toughened with PHAs were rougher than that of their nontoughened counterparts. The ternary PLA-based WPCs exhibited ductile fracture during mechanical testing. Differential scanning calorimetry (DSC) showed that addition of PHAs into the composites caused deviations of the cold crystallization temperature and melting temperature of PLA. Thermogravimetric analysis indicated that the PHAs reduced the thermal stability of the PLA-based WPCs. PHAs can be a green toughening agent for PLA-based WPCs. The specific properties evidenced by the biocomposites may hint at their potential application, for example, in the automotive industry and civil engineering. © 2011 Wiley Periodicals, Inc. J Appl Polym Sci 124: 1831–1839, 2012

Key words: biodegradable; composites; injection molding; mechanical properties; toughness

INTRODUCTION

In recent years, the application of ecofriendly polymers has become more and more popular because of the global economic and environmental issues resulting from the overuse of synthetic nondegradable polymers.[1–4] Much attention has been paid to biodegradable polymers, most of which are biocompatible and sustainable in nature.[2] Among the numerous kinds of biodegradable polymers, polylactide [PLA; also called poly(lactic acid)] is a linear aliphatic thermoplastic polyester that is considered the most promising representative of the ecofriendly polymers.[5,6] However, the inherent brittleness and high cost of PLA impedes its large-scale commercial application.[7]

The addition of various modifiers, such as some rubbers,[8] plasticizers,[9] starches,[10] synthetic resins,[11–13] and various fibers,[14–16] into the PLA matrix have been widely investigated to increase the impact resistance of PLA. Among the PLA-based composites, blends modified with wood flour (WF) or fibers [often called *wood–plastic composites* (WPCs)] hold the greatest promise. WF has the advantages, over conventional inorganic fillers, of having a lower cost, lower density, and lesser abrasiveness to processing equipment.[17] To reduce the costs of composites and to tailor their properties, WF has been widely used as the filler for these green PLA-based WPCs.[18–20] Nowadays, PLA-based WPCs have earned a growing share in the market because they are completely biodegradable and renewable.[17–19] However, weak interfacial adhesion between the hydrophilic WF and the hydrophobic PLA and the uneven dispersion of WF in matrices usually lead to poor mechanical properties, especially impact strength.[15,17,21–23] Pilla et al.[17] modified recycled wood fiber (RWF) with silane to increase the compatibility of PLA and RWF. They found that the tensile strength of the molded PLA–RWF composites was independent of the RWF content, whereas the toughness and elongation at break decreased with RWF content. To improve the impact resistance of PLA-based WPCs, the addition of some toughening agents into the

Correspondence to: T. Qiang (qiangtao2005@163.com).
Contract grant sponsor: Education Department of Shaanxi Province of China; contract grant number: 09JK493.
Contract grant sponsor: Foundation of Xi'an Technological University; contract grant number: XAGDXJJ0809.

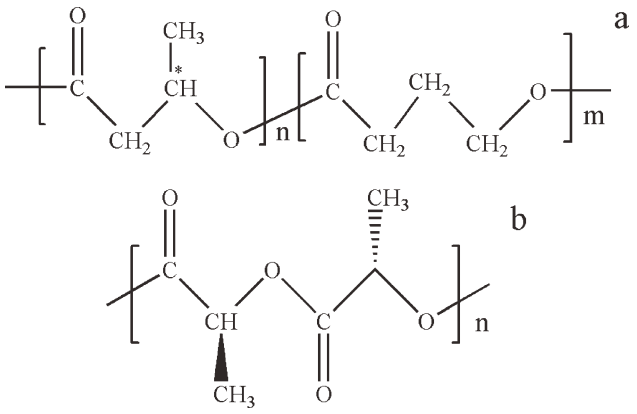

Figure 1 Chemical structures of (a) poly(3-HB-*co*-4-HB) (PHAs) and (b) PLA.

system is advisable. In our previous works, styrene–butadiene–styrene block copolymer was used as the toughening agent for PLA-based WPCs. However, WPCs toughened with styrene–butadiene–styrene are very difficult to degrade completely in the natural environment after they are transformed into waste. To our best knowledge, very few efforts have been made to improve the impact resistance of WF/PLA composites with degradable toughening agents.

Polyhydroxyalkanoates (PHAs) are a class of thermoplastic polyesters produced by microorganisms. PHAs share common assets with PLA in terms of their renewability and environmental degradability.[24] Takagi et al.[25] added elastic PHAs to brittle PLA to investigate the effects of PHAs on PLA. They found that the impact strength increased, and the blends were proven to be immiscible in the amorphous state. This made PHAs the preferred choice as the toughening agent in our PLA-based WPCs.

Therefore, in this study, we aimed to prepare and characterize completely biodegradable PLA-based WPCs with better impact resistance and to investigate the effects of PHAs on the mechanical and thermal properties and morphologies of the biocomposites.

EXPERIMENTAL

Materials

All of the raw materials were commercial grade. PLA (weight-average molecular weight = 100,000 g/mol) was obtained from BrightChina Industrial Co., Ltd. (Shenzhen, China). The copolymer of 3-hydroxybutyrate and 4-hydroxybutyrate [poly(3-HB-*co*-4-HB); grade EM5400F] was supplied by Ecoman Biotechnology Co., Ltd. (Shenzhen, China). The amount of 4-hydroxybutyrate in the copolymer was 12 wt %. Poly(3-HB-*co*-4-HB) (hereafter referred as PHAs) was used as the toughening agent for the PLA-based WPCs. The chemical structures of the PHAs and PLA are shown in Figure 1. Pine WF was obtained from Beijiao Hanguo Timber Co., Ltd. (Shunde, China).

Manufacture of the composites

The WF was dried at 110°C for 8 h in an oven to remove the moisture before compounding. Both the PLA and PHAs were dried at 80°C for 12 h. The properties of PLA/PHA blends were investigated by Noda et al.[26] in their previous research. They found that PHAs could be homogeneously dispersed in these blends at a relatively low level (i.e., 20 wt %). The content of PHAs in our PLA-based WPCs was determined to be 25 wt % to obtain the optimum impact resistance, on the basis of the results of Noda et al.'s[26] research. The four typical compositions of the PLA-based WPCs are illustrated in Table I.

The mixture of the PLA, WF, and PHAs was done by mechanical mixing method with a high-speed mixer (SHR-50A, Huaming Machinery Co., Ltd., Zhangjiagang, Jiangsu, China) at 1500 rpm for 5 min. Then, the initial mixture was melt-mixed in an extruder [TE-35, Coperion (Nanjing) Machinery Co., Ltd., Jiangsu, China] at a mixing speed of 400 rpm with a temperature profile of 135, 140, and 145°C and 140°C for the die. The extruder was equipped with intermeshing conical twin screws, the length-to-diameter ratio of which was 38. The molten compounded strands were immediately cooled to room temperature with water and were then cut into grains with a granulator (QLJ-1, Mingsu Machinery Co., Ltd., Zhangjiagang, Jiangsu, China).

The extrusive grains were dried at 110°C for 8 h and were then fed into an injection-molding machine (JM268-C^2, Chenhsong Machinery Co., Ltd., Hong Kong) to mold test bars. The following temperatures were set at respective zones for injection molding: 140°C near the feeder, 145°C in the middle zone(s), and 135°C for the nozzle. A pack/hold pressure of 6.5 MPa was used during the injection molding. To ensure complete mold filling, the pack and hold time were set as 15 and 5 s, respectively. The mold was maintained at room temperature to allow adequate cooling of the molded parts. A cooling time of 30 s was provided to ensure that the parts did not break during die separation. The tensile bars

TABLE I
Representative Compositions of the PLA-Based WPCs

Sample code	Relative content (wt %)		
	PLA	WF	PHAs
Sample 1	80	20	0
Sample 2	65	10	25
Sample 3	55	20	25
Sample 4	45	30	25

were tagged as type I, and the impact bars were notched according to GB/T 16421-1996 and GB/T 16420-1996.

Mechanical behaviors

A universal tester (T-10A, Reger Instrument Co., Ltd., Shenzhen, China) and an impact tester (XJJD-5, Jinjian Testing Instrument Co., Ltd., Chengde, China) were used to test the tensile and Charpy impact strengths of the injection-molded bars according to GB/T 16421-1996 and GB/T 16420-1996, respectively. The injection-molded bars were conditioned at 50 ± 10% relative humidity and 23 ± 2°C in a walk-in conditioning room for 48 h before testing. Five valid tensile and impact bars were tested for each composition, and the averages of the tested samples was taken for the results. The speed of the moving clamps was 50 mm/min during the tensile test.

Morphology of the fracture surface

The morphologies of the WF, PHAs, and cryofractured (by liquid nitrogen) surfaces of pure PLA and their binary and ternary notched impact bars were characterized by a S2700 scanning electron microscope (Hitachi, Japan, Xi'an, China). All of the fracture surfaces were observed after they were coated with a layer of gold in an ion-sputtering coater (SBC 12, KYKY Technology Development Co., Ltd., Beijing, China) to prevent charging during the scanning electron microscopy (SEM) investigation.

Thermal characterization

The thermal properties of the test samples were investigated with simultaneous thermogravimetric analysis (TGA)/differential scanning calorimetry (DSC; TA Instruments, SDT Q600, Xi'an, China), which could simultaneously record the results of DSC and TGA. We collected the data by heating the specimen in a single step from 50 to 400°C in air at a constant heating rate of 10°C/min. The number of each investigated samples for thermal analysis was 3. The most typical one among the three curves was selected to illustrate in the following section.

RESULTS AND DISCUSSION

Mechanical properties

Figure 2 shows the stress–strain curves of pure PLA and the four typical PLA-based WPCs. The breaking strength of pure PLA was 67.14 ± 0.88 MPa, and its stress–strain curve showed hard and brittle features without evidence of plasticity; this confirmed its inherent brittleness. The elongation at break of sample 1 was only 6.7 ± 0.8% (minimal among the five investigated bars), and its breaking strength decreased to 45.03 ± 1.34 MPa; this suggested that the interfacial adhesion between PLA and WF was very weak. The elongations at break of samples 2 and 3 increased slightly compared with that of sample 1, but the samples still showed hard and brittle features similar to those of pure PLA. It could be seen that sample 4 showed distinct yielding and necking phenomena during the tensile process. The substantial plastic deformation revealed that sample 4 exhibited ductile fracture after yielding during the tensile process. The elongation at break of sample 4 was three times that of pure PLA. These results suggest that there were different types of deformation mechanisms for sample 4 and sample 1–3. Obviously, the failure of sample 4 was highly localized and did not result in catastrophic breakdown. The fracture strengths of samples 2–4 decreased to about 45% of that of the pure PLA. The two-ordered polynomial regression between the tensile strength and the composition of the investigated samples was conducted. It was found that the tensile strength (Y) and the relative content of PLA (X) of the investigated samples fit the following two-ordered polynomial: $Y = 173.32X^2 - 184.97X + 79.5$ ($R^2 = 0.9862$). The result shows that the tensile strength of the PLA-based WPCs was mainly determined by the PLA content.

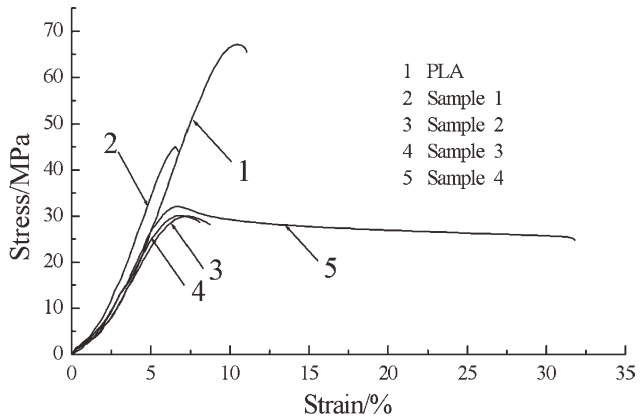

Figure 2 Typical stress–strain curves of the pure PLA and PLA-based WPCs. The number of each investigated samples for the impact test was 5. The average value and standard deviation of the respective yield strength and elongation at break were 67.14 ± 0.88 MPa and 11.1 ± 1.2% for PLA, 45.03 ± 1.34 MPa and 6.7 ± 0.8% for sample 1, 29.97 ± 0.75 MPa and 8.7 ± 0.9% for sample 2, 30.11 ± 1.15 MPa and 8.1 ± 1.1% for sample 3, and 32.10 ± 0.68 MPa and 31.8 ± 0.7% for sample 4, respectively.

The tensile properties for our PLA-based WPCs were inconsistent with those of Pilla et al.[17] This was attributed to five factors: differences in the granular shapes of PLA (pellet vs sphere), fillers [recycled wood fiber (RWF) vs pine WF], WF pretreatments

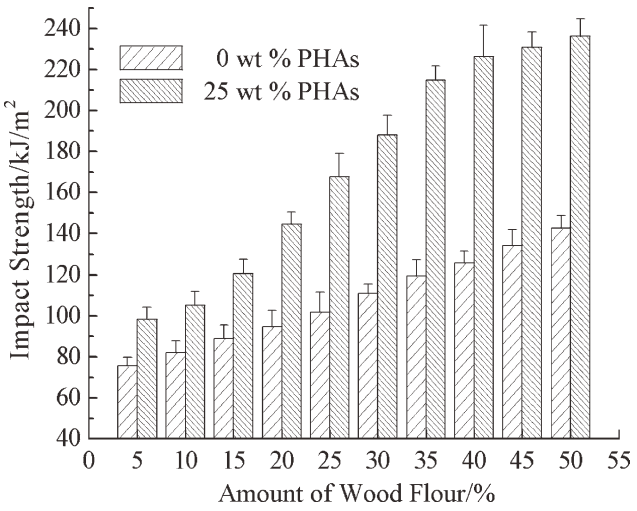

Figure 3 Impact strength of the PLA-based WPCs toughened with and without PHAs. The number of each investigated sample for the impact test was 5.

(treated with silane, coupling agent, and 0.5% RWF content vs untreated), toughening agents (with vs without PHAs), processing methods (kinetic mixing and injection molding vs mechanical mixing and extrusion blending followed by injection molding), and temperatures of the injection-molding process (average temperature of 204.3°C at respective zones vs average temperature of 140°C).

Figure 3 shows the impact strength of the PLA-based WPCs toughened with and without PHAs. The impact strength of sample 2 was 105.31 ± 6.64 kJ/m^2, whereas that of sample 1 was only 94.69 ± 7.98 kJ/m^2 (i.e., an 11.2% relative increase). It could be further found that the impact resistance of the PLA-based WPCs toughened with PHAs was higher than that of their nontoughened counterpart. The better interfacial adhesion between PLA and WF may have been formed within the PHAs-toughened WPCs. The improvement of the impact strength of the ternary PLA-based WPCs was attributed to the toughening agent PHAs. The inclusion of the elastic PHAs in the binary PLA/WF composites greatly improved their impact resistance, which was similar to that of high-impact polystyrene (PS) toughened with rubber.[26]

Interestingly, the slopes of the impact resistance to the WF content for the PLA-based WPCs toughened with and without PHAs were different, although both of them increased with WF content (see Fig. 3). The impact strength of the nontoughened PLA-based WPCs increased slowly, with approximately the same slope when the amount of WF increased from 5 to 50 wt %. The impact strength of the PLA-based WPCs toughened with PHAs also increased slowly, with approximately the same slope when the content of WF was less than 15 wt % or more than 35 wt %. However, the slope of the curve increased significantly when the amount of WF was between 15 and 35 wt %. They manifested a brittle fracture when the amount of WF was lower than 15 wt % and a ductile fracture when it was above 35 wt %; this was further confirmed by the following results from the morphologies of the fracture surfaces. That is, there was a brittle–ductile transition (BDT) of the impact strength for the PLA-based WPCs toughened with PHAs when the amount of WF was between 15 and 35 wt %. The curve of the impact resistance to the WF content is called the master curve of BDT, which is the proof of BDT for the mechanical properties of materials.

The percolation phenomenon is widely used to describe the insulator-to-conductor transitions of composites with conductive fillers and insulating matrices.[27–32] Percolation theories have been applied to describe the BDTs of composites modified with elastomer.[33,34] The percolation model was used by Margolina and Wu[34] and Guo et al.[35] to investigate nylon/rubber blends and PS/polyolefin elastomer (POE) blends, respectively. According to Guo et al.,[35] the percolation threshold of the POE content for BDT was 14 wt % in the PS/POE blends. In this investigation, the percolation transition behavior of the impact strength–WF content for the PHAs-toughened WPCs occurred when the amount of WF was between 15 and 35 wt %. The percolation threshold of the WF content for BDT in our PLA-based WPCs toughened with PHAs was 15 wt %, which was close to the POE content in the PS/POE blends.

Morphology

Figures 4 and 5 show the scanning electronic micrographs of the WF, PHAs, and cryofractured surfaces of the pure PLA, PHAs/PLA and WF/PLA blends, and sample 1; these provide a clue to the improvements of the mechanical properties for the PLA-based WPCs toughened with PHAs. The pine WF was in particle form, and the particulate size was about 10 μm, with an aspect ratio of about 1–4 [Fig. 4(a)]. The PHAs were in spherical form, and their average dimensions were in the range 0.5–1 μm [Fig. 4(b)]. The injection-molded bars of pure PLA showed the typical brittle fracture during the cryofracturing process; this could be concluded from the glossy and ordered morphologies of the fracture surface. Moreover, there were some distinct river markings on the fracture surface of the pure PLA [Fig. 4(c)]. The cryofractured surface of the binary PHAs/PLA blends had some spherical pores, with an average size of less than 0.5 μm; these were attributed to the phase-separated PHAs [Fig. 5(a)]. This result was consistent with Takagi et al.'s[25] research. The relative content of PHAs in the PHAs/PLA blends was 20 wt %. For the binary WF/PHAs blends, there were some features of WF and its traces [Fig. 5(b)].

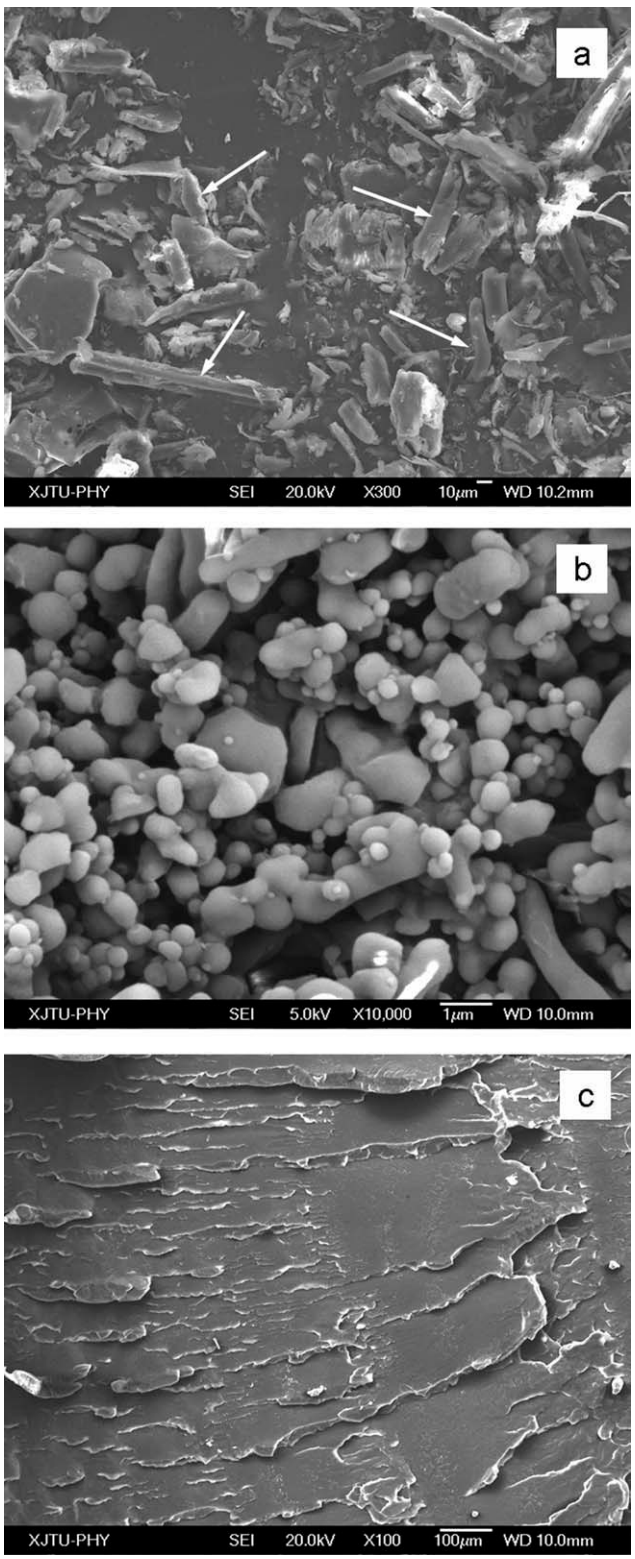

Figure 4 SEM images of the (a) WF and (b) PHA, and (c) the fracture surface of pure PLA. The arrows indicate the WF particles.

Pores with average size of about 0.5 μm could be observed all over the fracture surfaces. In these WF/PHAs blends, the content of WF was 20 wt %.

The fracture surface of sample 1 was rather smooth [Fig. 5(c)], whereas those of samples 2–4 were rougher [Fig. 6(a–c), respectively]. Several WF particles could be observed in the micrographs of samples 2–4, some of which were pulled out from the surface of the ternary WPCs during the cryofracturing process. At the same time, the cross-sectional surfaces of samples 2–4 [Fig. 6(a–c)] showed some distinct characteristics compared to sample 1 [Fig. 5(c)]. The fracture interfaces of samples 2–4 were fuzzier, and fewer traces of WF pullout were observed. Moreover, we found that the traces of sample 4 were fewest among samples 2–4, although the content of WF was the highest. The cohesive surface of sample 4 showed some features of ductile fracture; this was further evidence that the PLA-based WPCs toughened with PHAs had better impact resistance.

The decrease in the pullout of WF from the WPCs increased the mechanical properties of the composites when the content of WF was increased. At the same time, there may have been mechanical interlocking between the PLA and WF. Good mechanical interlocking between PLA and WF was attributed to the surface roughness of WF by Shah et al.[20] in their previous study. However, Noda et al.[26] found that PHAs could not crystallize fully when they were finely dispersed in the PLA matrix at a low level (i.e., 20 wt %). The SEM images showed that there was phase separation in the binary PHAs/PLA blends [Fig. 5(a)], which could partly explain the unexpected increase in the effective toughness of such PLA/PHAs blends. A comparison of the morphologies of the fracture surfaces of the ternary composites with those of the binary blends suggested that our ternary PLA-based WPCs were similar to the discussed PLA/PHAs blends. We deduced that the good mechanical interlocking between PLA and WF in our PLA-based WPCs was due to the toughening agent (i.e., PHAs). PHAs played an important role in the microstructural evolution of the composites, which, in turn, improved the impact resistance of our PLA-based WPCs.

Thermal stability

The thermal properties of the raw materials and the PLA-based WPCs were studied with DSC. Figure 7 shows their DSC curves between 50 and 200°C. The glass-transition temperature (T_g), cold crystallization temperature (T_{cc}), melting temperature (T_m), cold crystallization enthalpy (ΔH_c), and melting enthalpy (ΔH_m) of pure PLA and the samples are summarized in Table II. ΔH_m of PLA in the PLA-based WPCs decreased compared to that of pure PLA. The decreasing ΔH_m could be ascribed to the reduction of PLA content in the samples. T_{cc} of sample 1 was

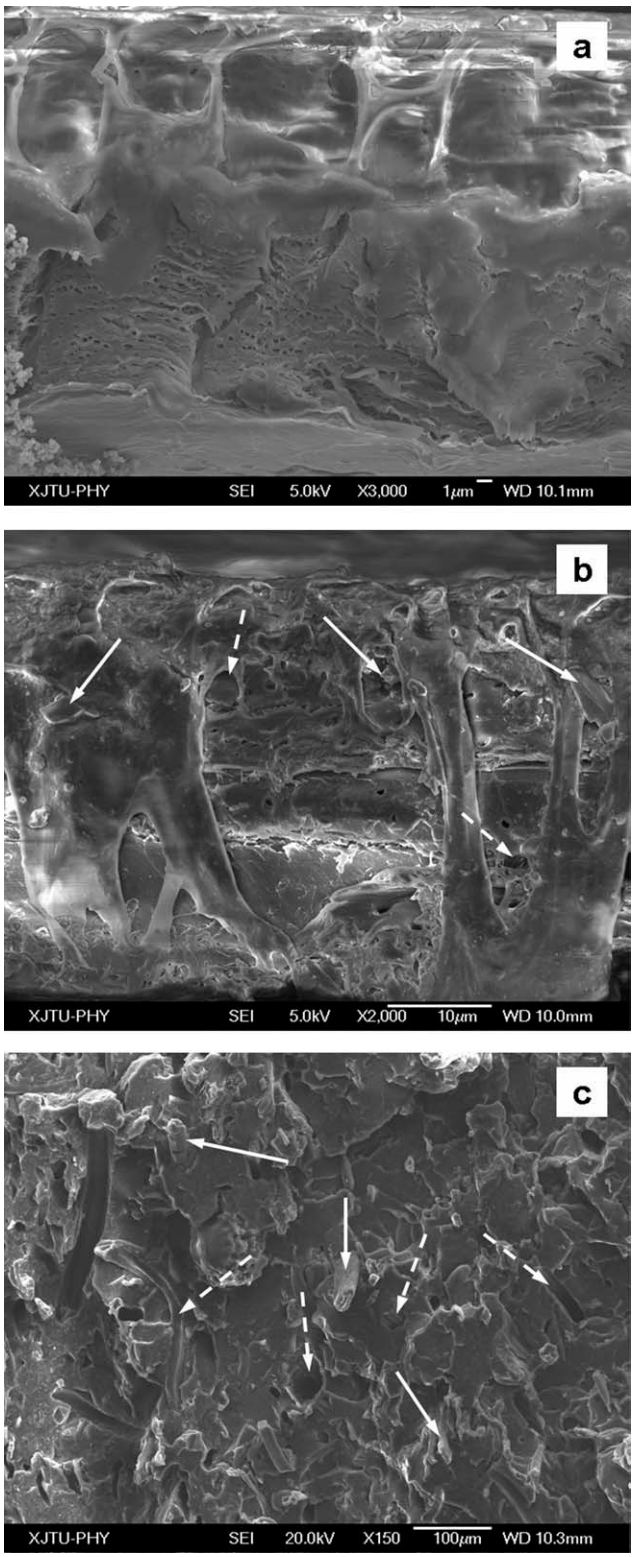

Figure 5 SEM images of the PHAs blends and WF/PLA composites. For the samples containing WF, the arrows indicate the WF particles, and the dotted arrows indicate the pullout of WF: (a) PHAs/PLA blends (80% PLA + 20% PHAs), (b) WF/PHAs blends (80% PHAs + 20% WF), and (c) sample 1 (80% PLA + 20% WF)

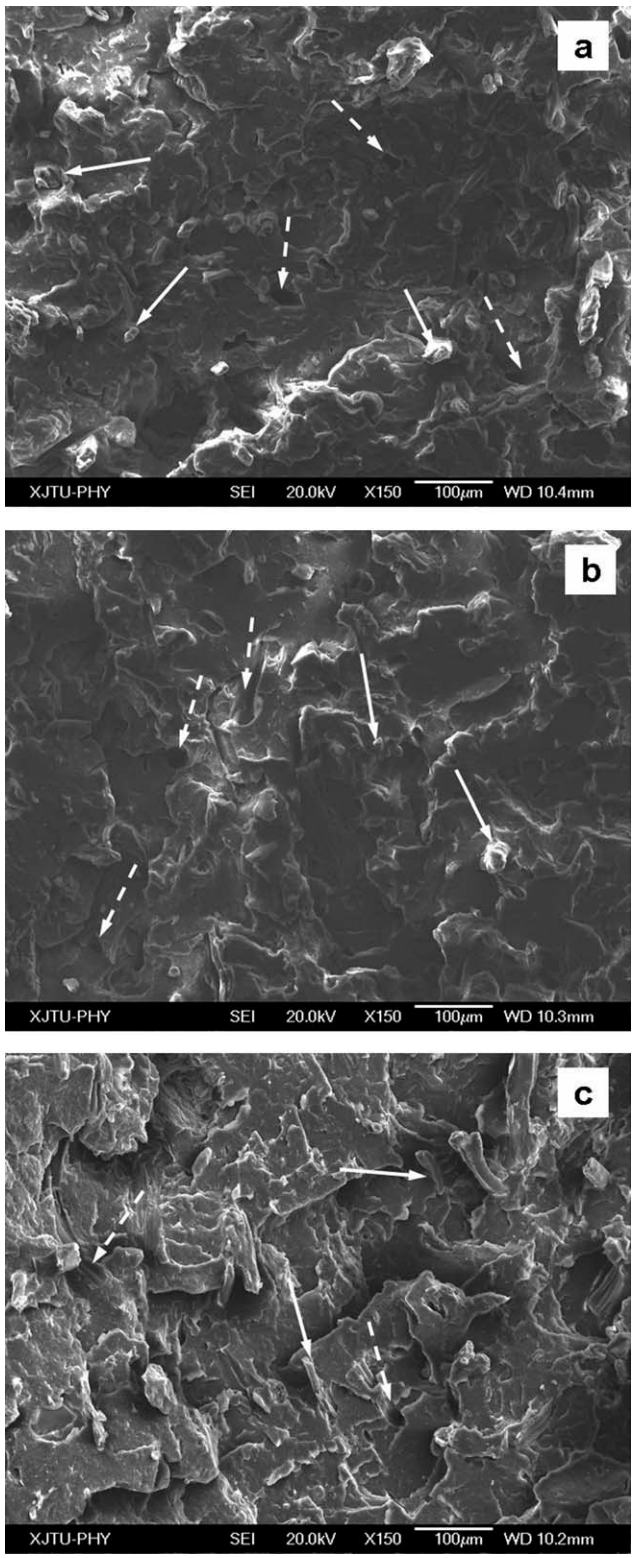

Figure 6 SEM images of the PLA-based WPC toughened with PHAs. The arrows indicate the WF particles, and the dotted arrows indicate the pullout of WF: (a) sample 2 (65% PLA + 10% WF + 25% PHAs), (b) sample 3 (55% PLA + 20% WF + 25% PHAs), and (c) sample 4 (45% PLA + 30% WF + 25% PHAs).

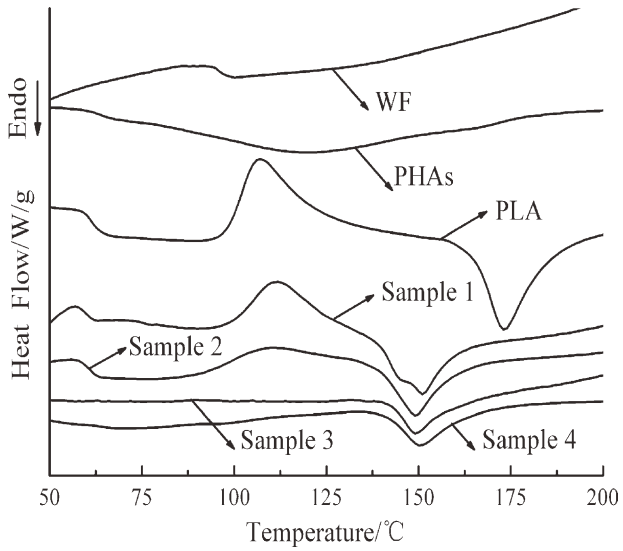

Figure 7 Melting curves of the raw materials and the PLA-based WPCs. The number of each investigated sample was 3. The most typical one among the three curves was selected to illustrate here.

higher than that of pure PLA. However, the cold crystallization peaks of samples 2–4 became less obvious. This indicated that there was no more amorphous region in these PLA-based WPCs that had the ability to crystallize during the heating process. As shown in Table II, the average T_m of the samples was 149.7°C. T_m decreased by about 23.5°C (i.e., a 13.6% relative decrease) for the PLA-based WPCs compared with that of pure PLA. Additionally, a double melting peak for sample 1 was observed at 146.2 ± 0.2 and 151.3 ± 0.2°C. The double-melting-peak behavior observed in sample 1 may have been due to two different types of crystalline structures obtained during the crystallization process,[36] which were due to the possible influence of WF.

The thermal stabilities of the raw materials and the PLA-based WPCs were investigated with TGA. Figure 8 shows the thermogravimetry (TG) curves of the raw materials and the samples between 200 and 400°C. The TG curves only illustrate above 200°C because there were no distinct differences below 200°C for the tested samples. The thermal stability of the PLA, WF, and PHAs could be determined from their TG curves. It could be seen that the 5, 25, 50, and 75% weight loss temperatures (T_5, T_{25}, T_{50}, and T_{75}, respectively) for pure PLA were 321, 346, 357, and 366°C, respectively. Moreover, the final decomposition temperature of the PHAs was lower than that of WF, although the onset decomposition temperature of the PHAs was, indeed, higher than that of WF. The thermal decomposition rates of the PLA, WF, and PHAs could also be obtained from their TG curves. These showed that the thermal decomposition rate of the PHAs was the fastest and that of PLA was the slowest among the three raw materials.

T_5, T_{25}, T_{50}, T_{75}, and the temperature at the maximum weight loss rate (T_p) of the samples are listed in Table III to illustrate the effect of the PHAs on the thermal stability of the PLA-based WPCs. The T_5, T_{25}, T_{50}, and T_{75} values of samples 3 and 4 were lower than those of sample 1. This indicated that the thermal stabilities of samples 3 and 4 were inferior to that of sample 1; this was due to the fastest decomposition rate of the PHAs. The thermal stability of sample 4 was worse than that of sample 3 because the relative content of WF in sample 4 (i.e., 30 wt %) was higher than that of sample 3 (i.e., 20 wt %). The general trend was that the addition of the PHAs to the PLA-based WPCs reduced the thermal stability of the biocomposites.

However, sample 2 was an apparent exception to the aforementioned rule. The T_5, T_{25}, T_{50}, and T_{75} values of sample 2 were the highest among the samples; this suggested that the PHAs could increase the thermal stability of the PLA-based WPCs when the content of WF was about 10 wt %. The thermal stability of sample 2 was even better than that of sample 1; this may have been due to the homogeneous dispersion and low loading of WF (i.e., 10 wt %) in sample 2, which could be further confirmed from the SEM images of samples 1 and 2 [Fig. 5(c) and 6(a)]. The low loading and homogeneous dispersion of WF in the PLA-based WPCs may have accounted for the improvement in their thermal stability.[15]

It is interesting to note that there was one stage of weight loss throughout the temperature range (i.e., 200–400°C) for samples 1 and 2, whereas there were two stages for samples 3 and 4. The weight loss

TABLE II
Thermal Characteristics of the Pure PLA and PLA-Based WPCs

Sample code	T_g (°C)	T_{cc} (°C)	T_m (°C)		ΔH_c (J/g)	ΔH_m (J/g)
			T_{m1}	T_{m2}		
PLA	61.3 ± 0.3	106.7 ± 0.1	173.2 ± 0.2		28.9 ± 0.6	36.6 ± 0.5
Sample 1	59.5 ± 0.2	111.1 ± 0.2	146.2 ± 0.2	151.3 ± 0.2	12.5 ± 0.3	33.2 ± 0.4
Sample 2	60.9 ± 0.3	—	149.6 ± 0.3		—	28.7 ± 0.2
Sample 3	60.3 ± 0.4	—	150.0 ± 0.2		—	26.8 ± 0.2
Sample 4	59.6 ± 0.2	—	151.3 ± 0.4		—	25.9 ± 0.3

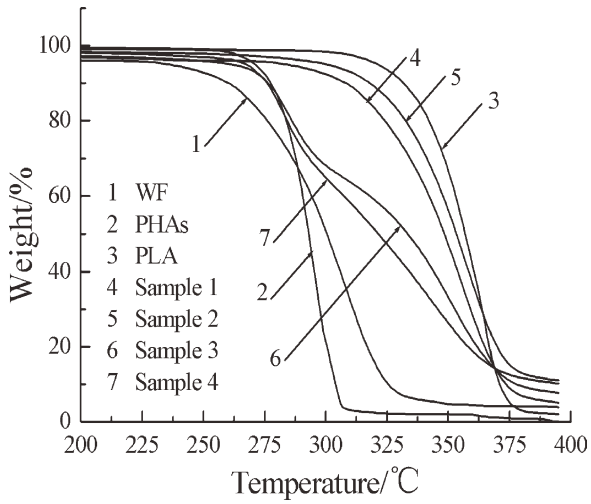

Figure 8 TG results of the raw materials and the PLA-based WPCs. The number of each investigated sample was 3. The most typical one among the three TG curves was selected to illustrate here.

peaks of samples 3 and 4 at about 285°C were similar to that of WF; this implied that excessive WF (i.e., 20 and 30 wt % for samples 3 and 4, respectively) was unfavorable for the thermal stability of the PLA-based WPCs toughened with PHAs.

CONCLUSIONS

Biobased and biodegradable WPCs composed of PLA (25–95 wt %), pine WF (5–50 wt %), and PHAs (0–25 wt %) were successfully prepared by extrusion blending followed by injection molding in this study. The mechanical and thermal properties and the morphologies of the composites were investigated by mechanical testing, thermal analysis, and observation of the fracture surfaces. The impact strength of the PHAs-toughened WPCs was improved at the cost of a reduction in the tensile strength. The PLA-based WPCs toughened with PHAs exhibited ductile fracture during tensile testing when the amount of WF was greater than 30 wt %,; this was further proven by the cryofractured features from SEM. A BDT of the impact strength for the PHAs-toughened WPCs was observed when the content of WF was between 15 and 35 wt %. The good mechanical interlocking between PLA and WF was primarily attributed to PHAs; this implied that PHAs was a good toughening agent for the PLA-based WPCs. DSC showed that the PHAs caused the deviations of T_{cc} and T_m of PLA in the PLA-based composites. TGA indicated that the addition of 25 wt % PHAs into the PLA-based WPCs reduced their thermal stability. The results demonstrate that PHAs can be used to tune the mechanical properties of the PLA-based WPCs. Furthermore, our research broadens the application of the percolation model in material science.

TABLE III
T_5, T_{25}, T_{50}, T_{75}, and T_p Values of the Pure PLA and PLA-Based WPCs

Sample code	T_5 (°C)	T_{25} (°C)	T_{50} (°C)	T_{75} (°C)	T_p (°C)	
					T_{p1} (°C)	T_{p2} (°C)
PLA	321	346	357	366	365	
Sample 1	284	330	348	362	357	
Sample 2	303	337	354	367	359	
Sample 3	261	291	334	358	285	351
Sample 4	267	288	322	351	284	345

The authors gracefully thank J. P. Zhang for her help in manufacturing the test samples, G. C. Zhang, Y. Z. Wang, Y. C. Xie, and W. X. Chen for their technical assistance, and Ph.D. candidate S. Liang for his help with thermal analysis. They are also grateful to all of the companies for donating the necessary raw materials.

References

1. Lei, H.; Pizzi, A.; Du, G. B. J Appl Polym Sci 2008, 107, 203.
2. Flieger, M.; Kantorova, M.; Prell, A.; Rezanka, T.; Votruba, J. Folia Microbiol 2003, 48, 27.
3. Madhavan, N. K.; Nair, N. R.; John, R. P. Bioresour Technol 2010, 101, 8493.
4. Luo, Y. F.; Wang, Z. Y.; Song, X. M.; Mao, Z. Z. Prog Chem 2008, 20, 1578.
5. Fortunati, E.; Armentano, I.; Iannoni, A.; Kenny, J. M. Polym Degrad Stab 2010, 95, 2200.
6. Sangwan, P.; Wu, D. Y. Macromol Biosci 2008, 8, 304.
7. Bhardwaj, R.; Mohanty, A. K. Biomacromolecules 2007, 8, 2476.
8. Ishida, S.; Nagasak, R.; Chino, K.; Dong, T.; Inoue, Y. J Appl Polym Sci 2009, 113, 558.
9. Murariu, M.; Ferreira, A. D. S.; Pluta, B. M.; Alexandre, L. M.; Dubois, P. Eur Polym J 2008, 44, 3842.
10. Sarazin, P.; Li, G.; Orts, W. J.; Favis, B. D. Polymer 2008, 49, 599.
11. Rasal, R. M.; Hirt, D. E. J Biomed Mater Res Part A 2009, 88, 1079.
12. Zhang, W.; Chen, L.; Zhang, Y. Polymer 2009, 50, 1311.
13. Wu, D.; Zhang, Y.; Zhang, M.; Zhou, W. Eur Polym J 2008, 44, 2171.
14. Suryanegara, L.; Nakagaito, A. N.; Yano, H. Compos Sci Technol 2009, 69, 1187.
15. Okubo, K.; Fujii, T.; Thostenson, E. T. Compos A 2009, 40, 469.
16. Graupner, N. J Compos Mater 2009, 43, 689.
17. Pilla, S.; Gong, S. Q.; O'Neill, E.; Yang, L. Q.; Rowell, R. M. J Appl Polym Sci 2009, 111, 37.
18. Bledzki, A. K.; Jaszkiewicz, A. Polimery 2008, 53, 564.
19. Ochi, S. Mech Mater 2008, 40, 446.
20. Shah, B. L.; Selke, S. E.; Walters, M. B.; Heiden, P. A. Polym Compos 2008, 29, 655.
21. Molnar, K.; Moczo, J.; Murariu, M.; Dubois, P.; Pukanszky, B. Express Polym Lett 2009, 3, 49.
22. Danyadi, L.; Renner, K.; Moczo, J.; Pukanszky, B. Polym Eng Sci 2007, 47, 1246.
23. Lee, H.; Kim, D. S. J Appl Polym Sci 2009, 111, 2769.
24. Araujo, A.; Lemos, A. F.; Ferreira, J. J Biomed Mater Res Part A 2009, 88, 916.

25. Takagi, Y.; Yasuda, R.; Yamaoka, M.; Yamane, T. J Appl Polym Sci 2004, 93, 2363.
26. Noda, I.; Satkowski, M. M.; Dowrey, A. E.; Marcott, C. Macromol Biosci 2004, 4, 269.
27. Poblete, V. H.; Alvarez, M. P.; Fuenzalida, V. M. Polym Compos 2009, 30, 328.
28. Li, W.; Liu, Z. Y.; Feng, J. M.; Yang, M. B. Acta Polym Sinica 2009, 40.
29. He, F.; Lau, S.; Chan, H. L.; Fan, F. Adv Mater 2009, 21, 710.
30. Hermant, M. C.; Klumperman, B.; Kyrylyuk, A. V.; Schoot, P. van der; Koning, C. E. Soft Matter 2009, 5, 878.
31. Wu, D. F.; Wu, L.; Yu, W.; Xu, B.; Zhang, M. Polym Int 2009, 58, 430.
32. Hermant, M. C.; Smeets, N.; Roger, C. F. van Hal; Meuldijk, J.; Heuts, H.; Klumperman, B.; van Herk, A. M.; Koning, C. E. E-Polymers 2009, 22.
33. Jiang, W.; Hu, Y. X.; Yin, J. H. J Polym Sci Part B: Polym Phys 2008, 46, 766.
34. Margolina, A.; Wu, S. Polymer 1988, 29, 2170.
35. Guo, Z.; Fang, Z.; Tong, L. Express Polym Lett 2007, 1, 37.
36. Carrasco, F.; Pagès, P.; Gámez-Pérez, J.; Santana, O. O.; Maspoch, M. L. Polym Degrad Stab 2010, 95, 116.